Perturbation of the Sun on Frozen Orbits Around Mars

Journal of Physics: Conference Series **1365** (2019) 012028 doi:10.1088/1742-6596/1365/1/012028

Perturbation of the Sun on Frozen Orbits Around Mars

A C Oliveira[1], R C Domingos[1], L M Silva[1], A F B A Prado[2] and D M Sanchez[2]

[1]Universidade Estadual Paulista (UNESP), São João da Boa Vista, SP
[2]Instituto Nacional de Pesquisas Espaciais (INPE), São José dos Campos, SP

E-mail: rita.domingos@unesp.br

Abstract. This work presents a study related to the perturbation of the Sun in the orbital evolution of artificial satellites on frozen orbits around Mars. The effect generated by the non-sphericity of Mars is considered. Frozen orbits are orbits that have the eccentricity and the argument of periapsis of the nominal orbit constant on average. Our goals are to verify how the gravity effect of the Sun affect such orbits and study their stability as a function of the parameters involved. We have performed numerical integrations considering different initial conditions for the frozen orbits. Using the method of the integral of the disturbing accelerations it is possible to calculate the magnitude of the total velocity variation due to each perturbation, as well as the degree and order of the most significant spherical harmonic over a long time. Our results showed that the effect of the perturbation of the Sun on the satellites depends on the initial values of eccentricity and semi-major axis of the orbit of the satellite.

1. Introduction

The scientific community has shown growing interest in exploring the planet Mars in the last five decades. Much has been studied about Mars due to the search for evidence of water and, consequently, life on the planet [1, 2]. Some missions have been directed at Mars, such as the US Mars Global Surveyor (MGS) [3] and Mars Reconnaissance Orbiter (MRO) [4].

In particular, the study of orbits around Mars is an important subject for mission planning. In general, studies related to orbits of artificial satellites around Mars consider the oblateness of the planet as the main factor influencing the orbit of the satellite [4]. However, the literature shows that artificial satellites in Martian orbits tend to undergo effects caused by the gravitational potential of the Sun [5]. Therefore, the presence of the Sun acting as a perturbing body should have an effect non-negligible on artificial satellites orbits because it can generate considerable effects on long time. In this context, this work presents a study of the gravitational perturbing of the Sun on frozen orbits of artificial satellites around Mars, considering also the effects generated by the non-sphericity of the planet. Therefore, in the present paper we considered different initial conditions for frozen orbits. Our goal is to verify how each perturbation could affect a satellite in a frozen orbit. Investigating the details these dynamical interactions is beyond the scope of the present work. Therefore, we will focus on the possible impact of the perturbing forces on the orbit of the satellite because the stability and survival of satellites around Mars is important for the success of missions, without investigating them in detail.

This work has the following structure. In Section 2, we present the initial conditions for the dynamical model used for the numerical integrations. The theory developed here is used to study the behavior of the satellite around Mars, where the Sun is the perturbing body. In Section 3, results and analysis of the numerical integrations are presented. Then, our final comments are made in the last section.

2. Dynamical Model and Initial Conditions

Our dynamic model is assumed to be a hypothetical system whose main body, the planet Mars, is assumed to be in the center of the reference system x-y. The perturbing body, the Sun, is in an elliptic orbit around the main body. The satellite, a massless body, is in orbit around the main body. The initial conditions are given with respect to the equatorial plane of Mars. To numerically integrate the orbital evolution of the artificial satellite around Mars, the equation of motion describing the dynamic model is given by [6]:

$$\ddot{\mathbf{r}} = -\frac{GM_M}{|\mathbf{r}|^3}\mathbf{r} + GM_{Sun}\left(\frac{\mathbf{r}_{Sun}-\mathbf{r}}{|\mathbf{r}_{Sun}-\mathbf{r}|^3}) - \frac{\mathbf{r}_{Sun}}{|\mathbf{r}_{Sun}|^3}\right) + \mathbf{P}_G \tag{1}$$

where G is the gravitational constant, M_M e M_{Sun} are the masses of Mars and the Sun, respectively, while $\boldsymbol{r}$ and $\boldsymbol{r}_{Sun}$ are the position vectors of the satellite and the Sun. In this case, the vector $\boldsymbol{P}_G$ represents the acceleration generated by non-sphericity of Mars, and depends directly on the gravitational potential of the planet, calculated using the fully normalized spherical harmonic coefficients of Mars. It is given by [6]:

$$\boldsymbol{P}_G = \sum_{m=0}^{M}\sum_{n=\eta}^{M} P_{G_{m,n,x}}\mathbf{i} + \sum_{m=0}^{M}\sum_{n=\eta}^{M} P_{G_{m,n,y}}\mathbf{j} + \sum_{m=0}^{M}\sum_{n=\eta}^{M} P_{G_{m,n,z}}\mathbf{k} \tag{2}$$

where M is the maximum value of n (degree) and m (order) for the harmonics to be considered, and depends directly on the term C_{nm} (spherical harmonic coefficient). In our numerical integrations, the value of M is assumed to be equal to 15 [7].

To calculate the individual contribution of each perturbation on the orbit of the satellite, we use the method of the integral of the disturbing accelerations (PI) [8]. In [6] is showed that this method allows us to calculate the magnitude of the variation of the velocity of the satellite due to each harmonic of the geopotential over time, as well as the variation of the velocity of the satellite over time due to each disturbing force. The expression for the variation of the velocity over time is given by:

$$PI_j = \frac{1}{T}\int_0^T |\mathbf{P}_j|\, dt \tag{3}$$

where PI_j, $\boldsymbol{P}_j$ and T correspond to the variation of velocity over time, perturbation of the Sun (or non-sphericity) and time interval of integration, respectively. It is important to say that the effect of each perturbation on the satellite is calculated by each of the forces individually, without being necessary to disregard other perturbations.

According to our goals, we focused on frozen orbits because they are characterized by keeping approximately constant the eccentricity (e) and the argument of periapsis (ω) of the nominal orbit, under the influence of the orbital perturbations [4, 9]. Therefore, the satellite crosses in a certain region always with the same altitude depending on the geographical location, bringing benefits through this regularity, such as mapping and monitoring certain areas of the planet. In recent decades, the frozen orbit configuration was used in missions such as the Seasat mission, the US/France TOPEX-Poseidon mission, and the European remote monitoring satellites ERS-1 and ERS-2.

The literature shows that the choice of initial values of e and ω must be adequate for given a semi-major axis (a) and inclination (i) values such that this combination of initial values corresponds to a frozen orbit [4]. In addition to the small variations of e and ω, frozen orbits are also advantageous because the initial values of a and i can be defined independently. For frozen orbits, the initial value of e is given by [4]:

$$e = -\frac{\frac{J_3 R}{2 J_2 a}\sin i \, \sin\omega}{1 - \frac{3 J_2 R E}{a^2(5 \sin^2 i - 4)}} \tag{4}$$

where R is the planet's radius, J_2 and J_3 are the zonal harmonics of Mars dominant among the harmonic coefficients, and the value of E is given by:

$$E = (6 - \frac{169}{12}\sin^2 i + \frac{395}{48}\sin^4 i) - \frac{35 J_4}{18 J_2^2}(\frac{12}{7} - \frac{93}{14}\sin^2 i + \frac{21}{4}\sin^4 i) \tag{5}$$

Equation (4) shows that the positive sign of e strongly depends on the values of ω, J_2 and J_3. This may be a result of the fact that, the perturbation due to the non-sphericity can change significantly depending on those parameters. For the case of the Earth, for example, the most dominant term is J_2 with value of 1.082627×10^{-3}, and the values of the harmonic coefficients J_3 and J_4 are -2.53266×10^{-6} and -1.61962×10^{-6}, respectively. Thus, they have a significant effect on the determination of the frozen orbit. In this case, the value of ω should be 90°, since J_2 and J_3 have opposing signs. At Mars, the J_2 and J_3 perturbations are also dominant, with values equal to 1.9555×10^{-3} and 3.14498×10^{-5}, respectively, and they are important in the determination of the frozen orbit around Mars. For the case of Mars, the value of ω is 270° because J_2 and J_3 are both positives.

Taking Equations (4) and (5), the initial conditions of the satellites are obtained through a computational algorithm developed in C++ language, capable to find the values of e considering the combination of initial values a and i. Initial conditions of orbits with different values for the semi-major axis are found. Table 1 shows the initial conditions for seven frozen orbits considering $i = 50°$.

Table 1. Initial conditions of frozen orbits.

Satellite	a**(km)**	e
Orbit 1	8397	0.0024974
Orbit 2	13397	0.0015633
Orbit 3	18397	0.0011380
Orbit 4	23397	0.0008946
Orbit 5	28397	0.0007370
Orbit 6	33397	0.0006266
Orbit 7	38397	0.0005450

Evidently, as mentioned before, there is a wide range of values of a and i of frozen orbits to explore. However, in this work, we focused on the orbits shown in Table 1 In addition to that, the method of the integral depends on the specific orbit of the satellite and initial conditions of the perturbing body. Here we have focused on exploring the consequences of considering different orbital semi-major axis for the satellite. Thus, we have a single set of values of initial condition of the Sun and of the satellite starting at the Epoch January 1, 2025.

Using the conditions from Table 1, equations (1) and (3) are numerically integrated using the code written in Fortran language from [7], using Linux environment. The integration time is 15 terrestrial years, equivalent to approximately 8 orbital periods of Mars. The spherical harmonics are considered up to degree and order 15.

3. Results and Discussion

The results of the numerical integrations are shown in Figures 1 to 3, which refer to the variation of the eccentricity (Δe), semi-major axis (Δa), inclination (Δi), and argument of periapsis ($\Delta\omega$) as a function of the time for orbits 1, 3, and 5, respectively. Tables 2, 3, and 4 present a summary of the final results.

Figure 1 shows that, for orbit 1, e reaches variations of the order of 10^{-6}, while a presents variations of the order of 10^{-3}. With respect to the inclination, an oscillatory behavior is observed which represents small periodic variations of approximately $0,015°$. We can also see that ω suffers a variation of almost $-2,5°$. It can be noted that, after 15 terrestrial years, e and ω do not increase significantly.

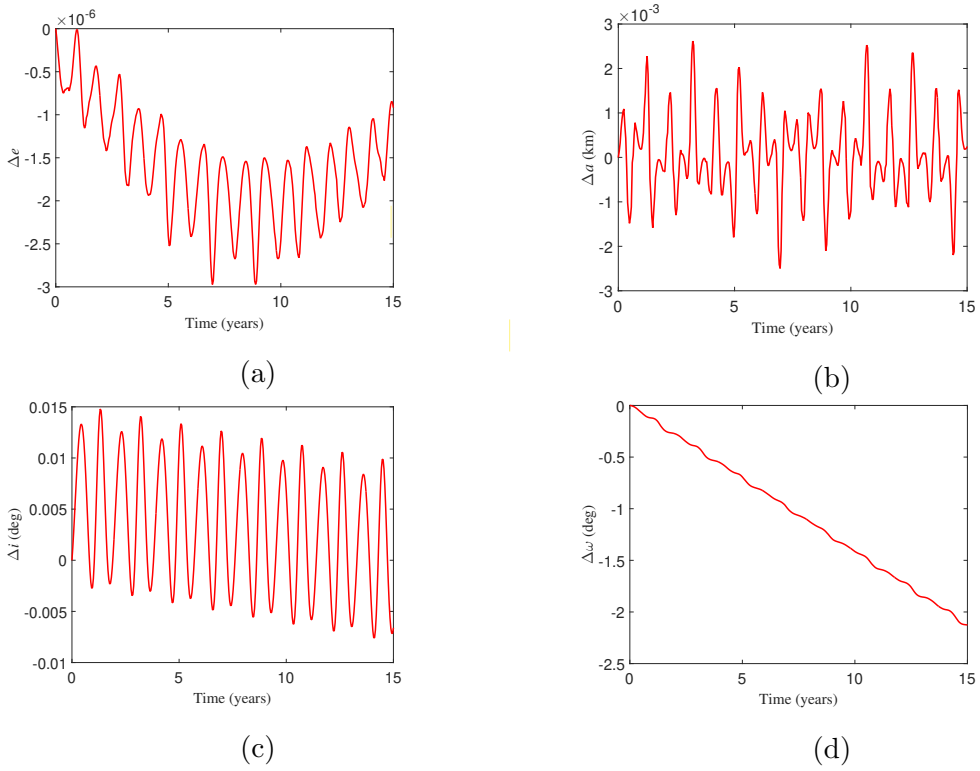

Figure 1. Variation of the orbital elements as a function of time for orbit 1 after 15 terrestrial years: (a) Δe (b) Δa (c) Δi and (d) $\Delta\omega$.

Figure 2 shows that, in the case of orbit 3, the eccentricity assumes a variation of the order of 10^{-5}. The semi-major axis variation does not have the same amplitude over time, but it can be said that it is periodic, because every 1.88 years the oscillatory behavior repeats itself. Then, it can be seen that, for 15 years (approximately 8 orbital periods of Mars, the variation of the semi-major axis has approximately 8 cycles, which indicates that the perturbation of the Sun is significant for each orbital period (remembering that 1 orbital period of Mars is $\sim$1.88 Earth years). The inclination presents an oscillatory behavior with small variations of, at the

most, about 0.06°. Analyzing the behavior of ω as a function of time, we can see that it has a variation $-7°$ for orbit 3.

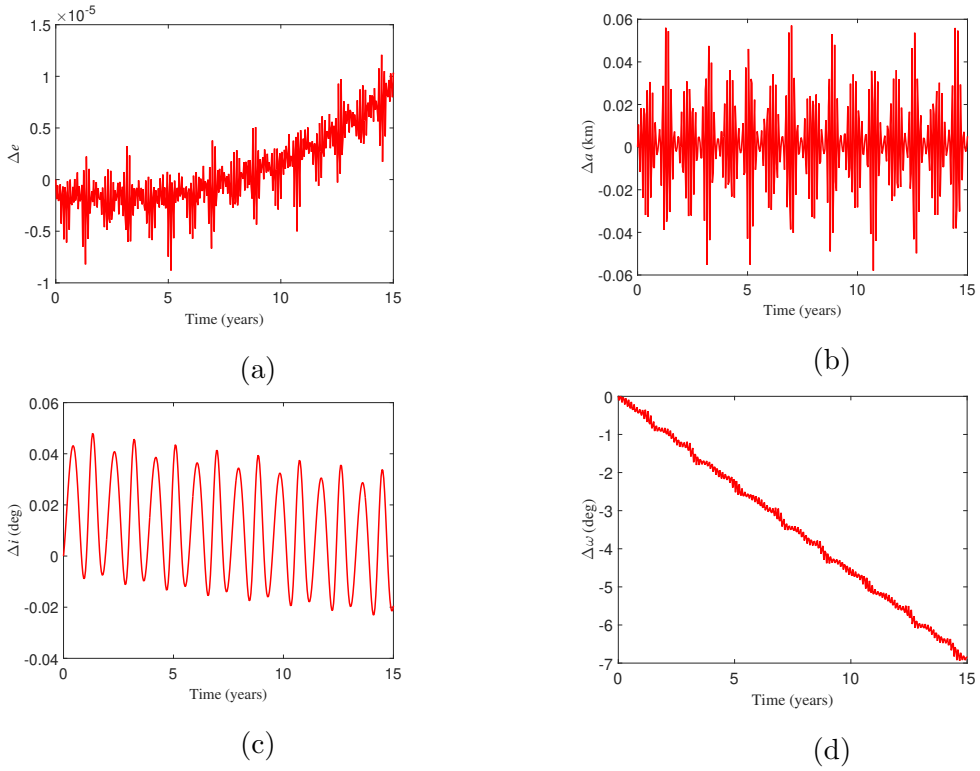

Figure 2. Variation of the orbital elements as a function of time for orbit 2 after 15 terrestrial years: (a) Δe (b) Δa (c) Δi and (d) $\Delta\omega$.

Figure 3 shows the results for orbit 5. By analyzing the orbital elements, we notice that the behavior of the variations is similar to that of orbit 3. In this case, the variation of a reaches a maximum of almost 0.35 km, while the change in the value of e is of the order of 10^{-5}. Regarding the inclination, an oscillatory behavior is observed, which represents small periodic variations of approximately 0.15°. We can also see that ω has a variation of approximately $-14°$.

In general, the behavior of the semi-major axis variations are similar for the cases analyzed in this study. It occurs around the average value. Using the method of the integral of the disturbing accelerations for each of the orbits, considering the interval of 15 years of integration, it is possible to obtain the magnitude of the variation of the velocity of the satellite due to the disturbing of the Sun (PI_S) and the non-sphericity (PI_G) over one orbital period of Mars. Table 2 presents the values of PI_S and PI_G for all orbits considered here.

Analyzing Table 2 it is possible to notice that PI_S has higher order of magnitude when compared to PI_G. Therefore, the perturbation of the Sun dominates the dynamics, which results in higher variation of the velocity of the satellite. It is also observed that the values of PI_S and PI_G depend on the values of the semi-major axis of the satellite. Thus, we can say that the dynamical behavior of the satellite is governed by the Sun.

As previously mentioned, our numerical integrations have been performed using spherical harmonics up to degree and order 15. Considering that the effects of the perturbations are cumulative, numerical integrations for each orbit are done for an integration time equal to 100 terrestrial years. The value of the magnitude of PI_G is measured when varying the maximum value (M) of the degree and order of the spherical harmonics. In particular, our main interest is

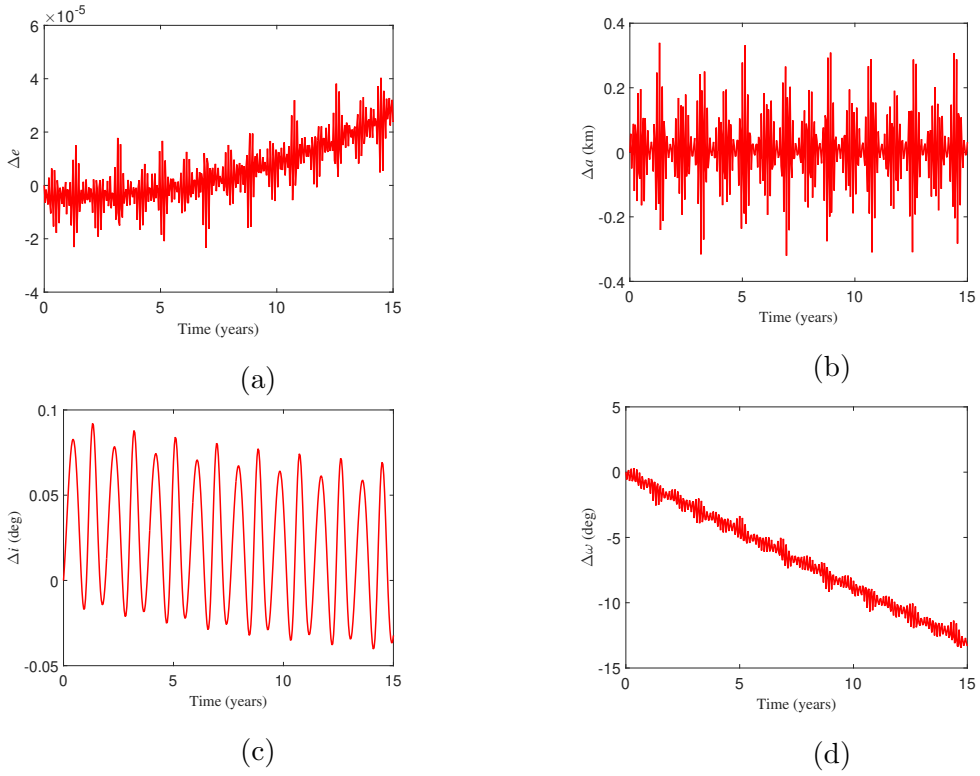

Figure 3. Variation of the orbital elements as a function of time for orbit 3 after 15 terrestrial years: (a) Δe (b) Δa (c) Δi and (d) $\Delta\omega$.

Table 2. $PI_S(m/s)$ and $PI_G(m/s)$ over one orbital period of Mars.

Satellite	$\boldsymbol{a}$**(km)**	PI_S	PI_G
Orbit 1	8397	7.4149581×10^{-4}	1.9867190×10^{-11}
Orbit 2	13397	1.1824448×10^{-3}	3.0649359×10^{-12}
Orbit 3	18397	1.6261559×10^{-3}	8.5606361×10^{-13}
Orbit 4	23397	2.0652911×10^{-3}	3.2952097×10^{-13}
Orbit 5	28397	2.5064316×10^{-3}	1.5188852×10^{-13}
Orbit 6	33397	2.9477510×10^{-3}	7.9376391×10^{-14}
Orbit 7	38397	3.3891982×10^{-3}	4.5437539×10^{-14}

to determine the maximum quantity of spherical harmonics that could be considered significant for this type of study. The results are shown in Tables 3 and 4, where the values of M and PI_G are presented for each orbit, respectively. It can be noted that the values of PI_G become constant from M equal to 7 up to 15. Then, to consider maximum values of degree (n) and order (m) equal to 7 is sufficient for the study presented here.

The results also showed that the perturbations due to the terms related to harmonics up to degree and order 2 are the most significant, that is, for pairs (n, m) equal to $(2, 0)$ and $(2, 2)$. These values of variations of velocities produced by the non-sphericity of Mars are the most significant and very close in order of magnitude. These values are presented in Table 5.

Table 3. $PI_G(m/s)$ over one orbital period of Mars for M until 15, in 100 terrestrial years.

M	$PI_{G(Orbit1)}$ $(\times 10^{-11})$	$PI_{G(Orbit2)}$ $(\times 10^{-12})$	$PI_{G(Orbit3)}$ $(\times 10^{-13})$	$PI_{G(Orbit4)}$ $(\times 10^{-13})$
2	1.7692060	2.7300959	7.6765193	2.9355723
3	1.7692060	2.7300959	7.6765193	2.9355723
4	1.7692060	2.7300959	7.6765193	2.9355723
5	1.7692354	2.7301248	7.6765792	2.9355907
6	1.7692354	2.7301248	7.6765792	2.9355907
7	1.7692352	3.0735458	8.6434711	3.3046866
8	1.7692352	3.0735458	8.6434711	3.3046866
9	1.9919588	3.0735962	8.6435743	3.3047175
10	1.9919588	3.0735962	8.6435743	3.3047175
11	1.9919588	3.0735962	8.6435743	3.3047175
12	1.9919588	3.0735962	8.6435743	3.3047175
13	1.9919588	3.0735962	8.6435743	3.3047175
14	1.9919588	3.0735962	8.6435743	3.3047175
15	1.9919588	3.0735962	8.6435743	3.3047175

Table 4. $PI_G(m/s)$ over one orbital period of Mars for M until 15, in 100 terrestrial years.

M	$PI_{G(Orbit5)}$ $(\times 10^{-13})$	$PI_{G(Orbit6)}$ $(\times 10^{-14})$	$PI_{G(Orbit7)}$ $(\times 10^{-14})$
2	1.3531413	7.0771539	4.0545907
3	1.3531413	7.0771539	4.0545907
4	1.3531413	7.0771539	4.0545907
5	1.3531484	7.0771856	4.0546069
6	1.3531484	7.0771856	4.0546069
7	1.5231956	7.9656437	4.5625798
8	1.5231956	7.9656437	4.5625798
9	1.5232074	7.9656958	4.5626057
10	1.5232074	7.9656958	4.5626059
11	1.5232074	7.9656958	4.5626059
12	1.5232074	7.9656958	4.5626059
13	1.5232074	7.9656958	4.5626059
14	1.5232074	7.9656958	4.5626059
15	1.5232074	7.9656958	4.5626059

4. Final Remarks

Looking at the results obtained, it was possible to observe that the effects generated by the perturbation of the Sun and the non-sphericity of Mars are directly related to the initial conditions of the satellite. The behavior of the inclination and semi-major axis variations are similar for both cases studied in this work.

Analyzing the relation between stability and initial altitude of the satellite, it is noted that the magnitude of the variations of the orbital elements depend on the altitude of the satellite. So, a satellite on an orbit far enough from Mars shows that the effect of the non-sphericity is

Table 5. $PI_G(m/s)$ over one orbital period of Mars for (n, m) equal to $(2, 0)$ and $(2, 2)$, respectively, and PI_S.

Satellite	$PI_{G(2,0)}$	$PI_{G(2,2)}$	PI_S
Orbit 1	1.7691923×10^{-11}	2.2264736×10^{-12}	7.4236123×10^{-4}
Orbit 2	2.7300835×10^{-12}	3.4339787×10^{-13}	1.1834212×10^{-3}
Orbit 3	7.6764935×10^{-13}	9.6684452×10^{-14}	1.6257407×10^{-3}
Orbit 4	2.9355646×10^{-13}	3.6908157×10^{-14}	2.0674018×10^{-3}
Orbit 5	1.3531384×10^{-13}	1.7004180×10^{-14}	2.5097791×10^{-3}
Orbit 6	7.0771407×10^{-14}	8.8843401×10^{-15}	2.9513474×10^{-3}
Orbit 7	4.0545841×10^{-14}	5.0796104×10^{-15}	3.3936197×10^{-3}

negligible compared to the effect generated by the Sun, but the velocity variations generated by the non-sphericity of Mars must be taken into account, especially for longer time periods.

As previously mentioned, a frozen orbit keeps the eccentricity and the argument of periapsis approximately constant even in the face of perturbations. For the cases studied here, the results showed that, depending on the altitude, the satellite orbit tends to undergo to significant changes in the eccentricity and the argument of periapsis with respect to the initial orbit causing it to lose the conditions of a frozen orbit. Consequently, the satellite will not always pass in a certain region with the same altitude. The results also showed that considering degree and order of harmonics up to 7 is sufficient for this type of study.

5. Acknowledgment

The authors wish to express their appreciation for the financial support provided by São Paulo Research Foundation - FAPESP (grants #2014/22295-5 and 2016/24561-0) and National Council for Scientific and Technological Development - CNPq (grants #310317/2016-9, 800571/2016-9 and 406841/2016-0) and National Council for the Improvement of Higher Education – CAPES.

6. References

[1] Ojha L, BethWilhelm M, Murchie S L, McEwen A S, Wray J J, Hanley J, Massé M and Chojnacki M. 2015 Nat. Geosci. **8** 829
[2] Rapp D, Andriga J, Easter R, Smith J H, Wilson Y J, Clarck D L and Payne K. 2005 Aerospace Conference, IEEE. 10.1109/AERO.2005.1559325
[3] Jai B, Wenkert D, Hamme, B, Carlton M, Johnston D and Halbrook T. 2007 AIAA SPACE Conf. and Exposition, Long Beach, CA, AIAA Paper 2007-6090
[4] Liu X, Baoyin H and Ma X 2010 J. Guid. Con. Dyn. **33**(4) 1294
[5] Domingos R C, Silva L M, Dourado S C V, Prado A F B A. 2017 Dincon Conference Proceedings, São José do Rio Preto, SP, Brasil
[6] Sanchez D M, Prado A F B A and Yokoyama T. 2014 Advances Space Research **54** 1008
[7] Sanchez D M, Prado A F B A and Yokoyama T. 2015 Proc. of the 8th International Workshop on Satellite Constellations and Formation Flying, IWSCFF, p. 1-10
[8] Sanchez D M and Prado A F B A. 2018 Proc. of the AAS Astrodyn. Spec. Conf. **18** 320
[9] Liu X, Baoyin H and Ma X. 2011 Celest. Mech. Dyn. Astr. **109** 303